Extended Abstracts of the 2004 International Conference on Solid State Devices and Materials, Tokyo, 2004, pp. 898-899

G-9-3

Electric-Field-Controllable Spin Interferometer Based on the Rashba Spin-Orbit Interaction

Yoshiaki Sekine[1], Takaaki Koga[2,3], Junsaku Nitta[1,4]

[1]NTT Basic Research Laboratories, Nippon Telegraph and Telephone Corporation,
3-1 Morinosato-Wakamiya, Atsugi, Kanagawa 243-0198, Japan
[2]PRESTO, Japan Science and Technology Agency,
4-1-8 Honchou, Kawaguchi, Saitama 332-0012, Japan
[3]Graduate School of Information Science and Technology, Hokkaido University,
Kita 14, Nishi 9, Kita-ku, Sapporo, Hokkaido 060-0814, Japan
[4]CREST, Japan Science and Technology Agency,
4-1-8 Honchou, Kawaguchi, Saitama 332-0012, Japan

1. Introduction

In Spintronics [1,2], control of the spin degrees of freedom for carriers is under intensive investigation to find ways of making new devices, such as a spin field-effect transistor (spin FET) [3] and a spin interference device [4]. The Rashba spin-orbit interaction (SOI) [5,6], which is induced by the structural inversion asymmetry in a quantum well (QW), is a key to controlling the electron spin in semiconductors. Electric-field control of the Rashba SOI and estimation of the Rashba SOI parameter, α, have recently been achieved [7,8]. This success has stimulated us to make a spin interferometer. In the spin FET, injection of spin-polarized carriers from a ferromagnetic electrode is crucial. However, spin-polarized carriers are not necessary in the spin interferometer. This paper reports on the electric-field-controllable spin interferometer based on the Rashba SOI. The experimental results clearly demonstrate that the interference of the electron spin in an InGaAs QW can be controlled by means of the electric field.

2. Experiments

In this work, four samples which consists of an $In_{0.52}Al_{0.48}As/In_{0.53}Ga_{0.47}As/ In_{0.52}Al_{0.48}As$ QW are fabricated, and these samples have the same layer structure used in Ref. 8. Figure 1(a) shows a scanning electron microscope (SEM) image of the spin interferometer fabricated by the electron beam lithography and the ECR dry etching. In the lighter region, the InGaAs quantum well exists, and the darker region is etched. Each spin interferometer was etched into square-loop-shaped mesa, and many square-loop spin interferometers are arrayed. Figure 1(b) shows a schematic view of the Hall bar. The entire Hall bar was covered with a voltage-gate electrode, which makes it possible to control the Rashba SOI in the QW. Figure 1(c) shows a schematic view of the spin interferometer. The side length of the square loop, L_S, varies between 1.2 μm and 1.8 μm. In this work, the Al'tshuler-Aronov-Spivak (AAS) oscillations, which are due to the self-interference effect of two partial electron waves related by the time reversal operation [9], are measured in order to investigate the spin interference. In the AAS effect, an incident electron wave that comes to the square-loop spin interferometer splits into two partial electron waves. In the square-loop spin interferometer, one partial electron wave goes in the clockwise direction and the other goes in the counter-clockwise direction. Then, these two partial electron waves come back at the incident point and interfere each other. The paths of the two partial electron waves are completely same because of the time reversal operation. In Fig. 1(c), the electron paths for the AAS oscillations are depicted. The Aharonov-Bohm (AB) oscillations are also caused by the self-interference effect of the two partial electron waves [10], and electron paths for the AB oscillations are shown in Fig 1(d). In The AB effect, the two partial waves goes through half of the square loop and interfere each other. The electron-path lengths in the clockwise and the counter-clockwise directions are not completely same, so that phases of the AB oscillations among different spin interferometers are sample specific.

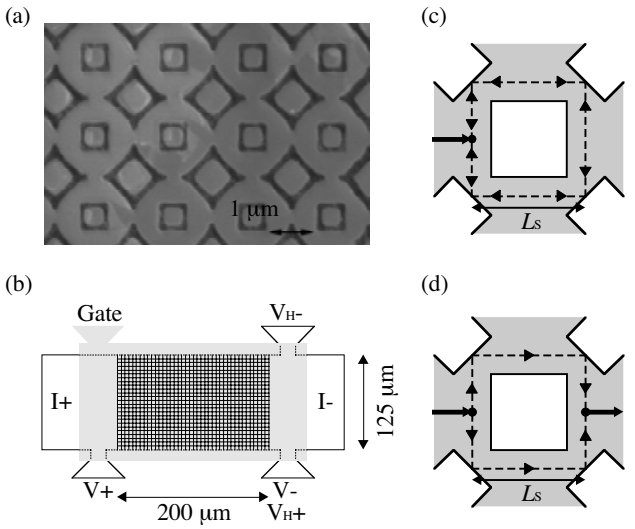

Figure 1(b) The SEM image of the sample. The lighter region is electron path and the darker region is etched. Many spin interferometers are arrayed. (b) The schematic view of the Hall bar. The gate electrode covers the entire Hall bar. The array of the spin interferometers is fabricated in the shaded area in order to measure the ensemble averaged conductivity. The number of the spin interferometers is more than 4000. (c) The schematic view of the spin interferometer. The incident electron splits into the two partial electron waves that go through the square loop. The electron paths of these two partial electron waves for the AAS oscillations are completely same. (d) The electron-path lengths of these two partial electron waves for the AB oscillations are not completely same.

The electric conductivity measurements for the four samples with various L_S were carried out by the four-probe method at 0.3 K. The ensemble averaged conductivity of many spin interferometers is investigated in order to measure the AAS oscillations. The AB oscillations and the universal conductance fluctuations [11] that are sample specific to each spin interferometer should be averaged out.

3. Experimental Result and Discussion

Figure 3(a) shows the electric conductivity σ_{xx} of the sample 4 (denoted in ref. 8) with L_S=1.4 μm as a function of the magnetic field B for gate voltages V_g of –1.2, -0.5, and 0 V at 0.3 K. Oscillations in σ_{xx} are observed. In order to extract the oscillatory part of σ_{xx}, the Fourier transformation analysis is applied. The oscillatory part of σ_{xx} after the Fourier transformation analysis, $\Delta\sigma_{xx}$, is presented in Fig. 3(b), and the oscillations are very clearly visible. The period of B of the oscillations corresponds to $(h/2e)/L_s^2$, which shows the oscillations are due to the AAS oscillations and the AB oscillations with the period of B of $(h/e)/L_s^2$ are averaged out.

The partial electron waves experience the spin precession due to the Rashba SOI while they travel through the square loop. In this work, ballistic transport of the electron through the each side of the square loop is assumed. So the spin precession angle θ at the each side of the loop caused by the Rashba SOI is written by the following equation,

$$\theta = 2\alpha m^* L_s / \hbar^2 \qquad (1).$$

Here, m^* is the electron effective mass. The presence of this spin precession results in a modulation of the amplitude of the AAS oscillations. This modulation has been theoretically calculated and the amplitude of the AAS oscillations, $A(\theta)$, is given by [12],

$$A(\theta) = -(\cos^4\theta + 4\cos\theta\sin^2\theta + \cos 2\theta)/4 \qquad (2).$$

This equation shows the details of the spin interference can be controlled by the α value that depends on the applied gate voltage. In Fig. 3, with increasing V_g, the sign of $\Delta\sigma_{xx}(B=0)$ changes from minus to plus. The amplitude of $\Delta\sigma_{xx}(B=0)=0$ corresponds to $A(\theta)=0$. From the equations (1) and (2), θ and α values at $\Delta\sigma_{xx}(B=0)=0$, where V_g is around –0.8 V, should be -0.424π and -0.782×10^{-12} eVm, respectively. This α value agrees well with α value deduced from the **k•p** perturbation theory [13] together with the potential profile of the QW obtained by the Poisson-Schrödinger self-consistent calculations. These results clearly show the details of the spin interference are controlled as expected theoretically by the applied gate voltage. In the other samples, the electric-field control of the spin interference was also confirmed.

4. Conclusion

By means of the gate voltage, the electron spin interference in the InGaAs QW was controlled by the Rashba SOI. The details of the spin interference were investigated from the amplitude of the AAS oscillations on the array of many interferometers. The gate dependence of the amplitude of the AAS oscillations coincided well with the gate dependence obtained from the theoretical calculation.

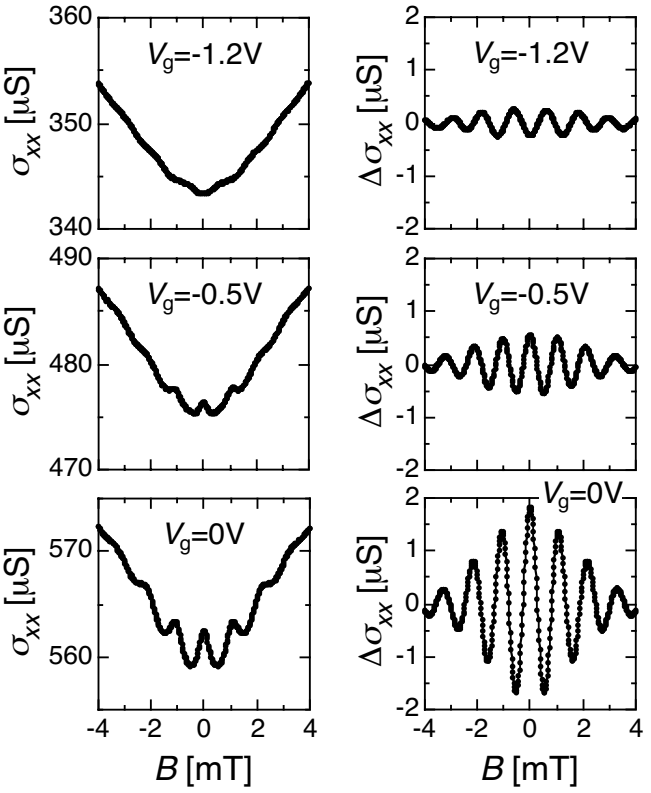

Figure 3(a) The electric conductivity σ_{xx} with L_s=1.4 μm as a function of the magnetic field B for gate voltages V_g of –1.2, -0.5, and 0 V at 0.3 K. (b) The oscillatory part of the electric conductivity $\Delta\sigma_{xx}$ as a function of B. The oscillations are clearly visible and only the AAS oscillations are observed. With increasing V_g, the $\Delta\sigma_{xx}$ at B=0 increases and the sign of $\Delta\sigma_{xx}(B=0)$ changes from minus to plus as expected theoretically. The spin interference is controlled by means of V_g.

References

[1] G. A. Printz, Phys. Today **48**, 58 (1995).
[2] *Semiconductor Spintronics and Quantum Computation*, eds. D. D. Awschalom, D. Loss, and N. Samarth, (Springer, Heidelberg, 2002)
[3] S. Datta and B. Das, Appl. Phys. Lett. **56**, 665 (1989).
[4] J. Nitta, F. E. Meijer, and H. Takayanagi, Appl. Phys. Lett. **75**, 695 (1999).
[5] E. I. Rashba, Sov. Phys. Solid State **2**, 1109 (1960).
[6] Y. A. Bychkov and E. I. Rashbba, J. Phys. C **17**, 6039 (1984).
[7] J. Nitta, T. Akazaki, H. Takayanagi, and T. Enoki, Phys. Rev. Lett. **78**, 1335 (1997).
[8] T. Koga, J. Nitta, T. Akazaki, and H. Takayanagi, Phys. Rev. Lett. **89**, 046801 (2002).
[9] B. L. Al'tshuler, A. G. Aronov, and B. Z. Spivak, JETP Lett. **33**, 94 (1981).
[10] Y. Aharonov and D. Bohm, Phys. Rev. **115**, 485 (1959).
[11] P. A. Lee and A. D. Stone, Phys. Rev. Lett. **55**, 1622 (1985).
[12] T. Koga, J. Nitta, and M. van Veenhuizen, to be published.
[13] Th. Schäpers, G. Engels, J. Lange, Th. Klocke, M. Hollfelder, and H. Lüth, J. Appl. Phys. **83**, 4324 (1998).